3D Simulation of Incompressible Poiseuille Flow through 180° Curved Duct of Square Cross-section under Effect of Thermal Buoyancy

Mourad Mokeddem[1], Houssem Laidoudi[1*], Oluwole Daniel Makinde[2], Mohamed Bouzit[1]

[1] Laboratory of Sciences and Marine Engineering, Faculty of Mechanical Engineering, University of Science and Technology of Oran - Mohamed Boudiaf, BP 1505, El-Menaouer, Oran 31000, Algeria
[2] Faculty of Military Science, Stellenbosch University, Private Bag X2, Saldanha 7395, South Africa
* Corresponding author, e-mail: houssem.laidoudi@univ-usto.dz

Abstract

In this paper, three-dimensional numerical simulations are carried out to investigate and analyze the gradual effects of thermal buoyancy strength on laminar flow of an incompressible viscous fluid and heat transfer rate inside a 180° curved channel of square cross-section. The governing equations of continuity, momentum and energy balance are obtained and solved numerically using finite volume method. The effect of Dean number, De, and Richardson number, Ri, on dimensionless velocity profiles and Nusselt number are examined for the conditions: De = 125 to 150, Ri = 0 to 2 at Pr = 1. The mean results are illustrated in terms of streamline and isotherm contours to interpret the flow behaviors and its effect on heat transfer rate. Dimensionless velocity profiles and the local Nusselt number at the angle 0° and 90° are presented and discussed. Also, the average Nusselt number on surfaces of curved duct is computed. The obtained results showed that by adding thermal buoyancy to computed domain, some early Dean vortices are observed at the angle 0° and new sort are observed at 90°. Furthermore, increase in Dean number increases the heat transfer rate. In other hand, increase in Richardson number decreases the average Nusselt number of 180° curved duct.

Keywords

mixed convection, 3D simulation, 180° curved duct, thermal buoyancy, Nusselt number

1 Introduction

The flow patterns and its effects on heat transfer in curved ducts have been investigated by huge number of researchers due to the complexities and critical importance of this kind of flow. Tremendous mechanical and chemical processing applications frequently confront a forced flow through a curved duct. Examples involving the flow inside tube type heat exchangers of high performance, refrigeration systems, oil refineries, device of food treatments, nuclear station, chemical process, etc. From analyzes of previous researches in this field [1-10], it was found that the flow patterns inside a curved tubes are completely different from the flow patterns through straights ducts. The presence of curved portion along the channel induces a centrifugal force of the flow and accordingly appearance of secondary flow in this part of channel. The deference of flow pressures between main flow and secondary flow create some vortices called Eckman vortices or end cells. This definition is given by Finlay and Nandakumar [1].

The exact descriptions of those vortices are given as pair of counter-rotating symmetrical vortices which appeared in channel cross-section. As all physical analytic of fluid flow phenomena, Dean [2] proposed for the first time a dimensionless number that used for controlling the flow stability through a curved duct, this number is called the Dean number, De, and it is given as:

$$De = \frac{u_m D_h}{v} \sqrt{\frac{D_h}{R_c}} \tag{1}$$

where U_m is mean velocity of the fluid flow through the channel, v is the kinematic viscosity, R_c is the radius of curvature and D_h is hydraulic diameter, it is given by Eq. (2):

$$D_h = \frac{4(\text{cross section area})}{\text{wetted perimeter}} \tag{2}$$

From the Dean number expression, it is evident that the instability of flow through a curved duct depends on large

number of fluid parameters and geometrical configurations such as the kind of fluid (Newtonian or non-Newtonian) [3-5], the duct cross-sectional form (circular [2], triangular [6], square [7-8], elliptical [9]), the value of curvature radius [10] and finally the external forces exerted on the flow as electromagnetic force [11]. For example the investigation of Dean [2] that is carried out for curved channel of circular cross-section showed that above the critical value of Dean number, new kind of counter-rotating vortices (pair) are observed to appeared on outer wall of duct. Those sorts of vortices are called Dean vortices.

For heat transfer thematic, there are some recent studies on the flow and heat transfer through a curved duct of different cross-sectional form. Rout et al. [6] numerically investigated a laminar flow and heat transfer of nanofluid in bend tube of triangular cross-section. The governing equations have been solved using commercial software ANSYS Fluent16. The effects of Reynolds number, volume fraction of fluid and aspect ratio on fluid patterns and heat transfer rate are the mean purpose of this study. It was found that using of nanofluid instead of basefluid enhances the heat transfer. Also, increase the aspect ratio of duct improves the heat transfer. Nayak et al. [12] performed in three-dimension the simulation of turbulent flow through U-tube of diameter 53 mm with radius ratios of 2.98 and 5.6 to predict the thermofluidic transport characteristics of the fluid in an 180° return bend of circular cross-section. The finite volume is used for numerical solving of governing equations. The RNG k-ε model is selected for numerical description of turbulent flow. The effects of Dean, Nusselt and Reynolds numbers on the vortex structure formations and heat transfer are studied in this work. It was found that a decrease in radius ratio of the curved tube increases the heat transfer. Soltanipour et al. [13] carried out the 3-D heat transfer simulations of ϒ-Al2O3/water nanofluid flow through a curved duct of square cross-section, the flow is assumed 3-D, steady, laminar and incompressible with constant proprieties. The cross-sectional walls of duct contain longitudinal ribs. The computational investigation is performed in order to test the effect of rib size, Dean number and particle volume fraction on heat transfer coefficient and Dean vortex appearance. The obtained results showed that presence of ribs on walls of duct enhance the total heat transfer coefficient of the duct. Nobari and Mehrabani [14] numerically studied the flow and heat transfer in curved eccentric annuli of circular cross-section. The governing equations are solved in three dimensions. The effects of eccentricity, Dean number, curvature and Prandtl number

on flow field and heat transfer characteristics was the main purpose of this investigation. It was shown that the eccentrically position of annuli could significantly improves the heat transfer rate. Ko [15] performed a numerical simulation of forced flow end entropy generation in 180° curved duct of rectangular cross-section supplied with longitudinal ribs. The investigations are done for 3-D laminar flow of steady regime. The effect of rib size, entropy generations and other physical parameters on secondary flow and heat transfer rate is analyzed in this work. The optimal rib size which induces the minimal entropy generation in the flow fields is found to be depended on the external heat flux and Dean number. Chandratilleke et al. [16] presented a numerical study for examining the secondary vortex motion and associated heat transfer process in fluid flow through a curved tube of rectangular cross-section. The simulations are carried out in three dimensions. The effect of fluidic parameters of hydrodynamic stability and heat transfer are shown in details. From critical analyses of those researches, it can be observed that forced convection heat transfer is the principal assumption used for the heat transportation, no attention has been devoted to mixed convection heat transfer and the effect of thermal buoyancy on fluid flow and heat transfer through the curved ducts of different cross-sectional from. Therefore, this paper tries to fill this gap in literature.

Indeed, mixed convection is the result of two paramount mechanisms. The first one is called the forced convection and it is occurred when forced flow brought on surface of heated area by some external devices such as a pump or blower. The second mechanism is called the natural convection and it is the motion of hot particles of fluid toward the upward direction due to density differences in the fluid occurring due to temperature gradient. This behavior is also known as the result of thermal buoyancy effect. The mixed convection refers to a scenario where both the flow inertial force and buoyant force interact with heat transfer rate. The principal parameter that controls the relative importance of forced and natural convection is the Richardson number (Ri), $Ri = Gr/\text{Re}^2$, where Gr is Grashof number and Re is Reynolds number. For $Ri < 1$, forced convection is the dominant process of heat transfer, for $Ri > 1$, natural convection is dominant. The forced and natural have an equal contribution of heat transfer at $Ri = 1$. Bouzit et al. [17] simulated through two-dimensional numerical investigation the effect of thermal buoyancy and rheological flow behavior of non-Newtonian flow inside a curved channel the governing equations are solved with the range

of following conditions: $Re = 40$ to 1000, $Ri = 0$ to 1 and $n = 0.4$ to 1.2 at fixed value of Prandtl number 0f $Pr = 7$. The results showed that some alternative vortices are seen to be appeared on duct walls and its number is seen to be increased with gradual increase in Richardson number as well as Reynolds number. This work can be considered as the first research treats the effect of thermal buoyancy on fluid transportation through a curved channel but it is limited only for two dimensional simulations. Other relevant published articles can be found in [18-24].

The above literatures revealed that no previous research is available on the combined effects of thermal buoyancy and Dean number on fluid flow and heat transfer characteristics through a 180° curved channel of square cross-section in three dimensional simulation. Therefore, the present study numerically examines the effects of Dean number and Richardson number on the flow pattern and heat transfer rate in a curved duct of square cross-section under the following parametric conditions as: $De = 125$ to 150, $Ri = 0$ to 2 at fixed $Pr = 1$. The obtained results are presented graphically and discussed.

2 Title Physical problem and governing equations

The Three-dimensional simulations of incompressible flow under the effect of thermal buoyancy inside a heated curved channel with square cross-section are here considered. Fig. 1 illustrates schematically the diagram of geometry with its physical problem. The considered geometry assembles three parts: in the beginning of geometry, an upstream channel of gap $H = R_2 - R_1$, width $l = H$ and length $L = 10H$, in the midst, a 180° bend channel with internal radius $R_1 = 14.6H$ and external radius $R_2 = 15.6H$ and at the end of geometry, a downstream channel containing the same dimensions as the upstream channel. The
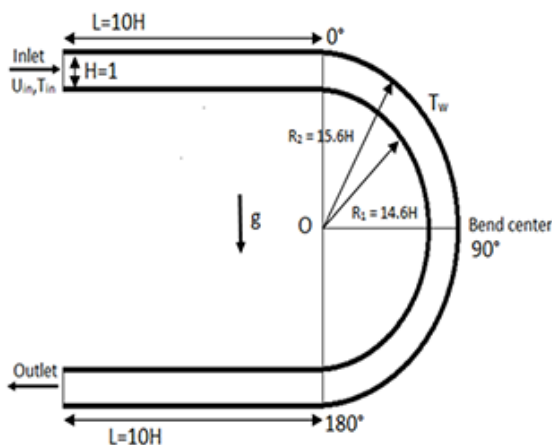

Fig. 1 Schematic diagram of the computational domain

geometrical dimensions of curved duct are selected from the previous research of Bara et al. [18]. The purpose of this work is to simulate the incompressible flow of viscous fluid through the curved channel under the effect of thermal buoyancy. Therefore, due to the computational considerations, the fluid flow enters the channel with free stream velocity U_{in} and temperature T_{in}. In order to investigate gradually the nature convection heat transfer from channel walls, the channel surfaces are kept higher temperature (T_w) than the free-stream temperature. $T_w > T_{in}$.

The thermo-physical proprieties are assumed to be independent of temperature except for density (ρ) manifesting in body force in the y-momentum equation. The steady dimensionless governing equations for this three-dimensional, laminar, incompressible, viscous flow with constant thermo-physical proprieties along with constant Boussinesq approximation and negligible dissipation effect can be defined in the following conservative forms Eq. (3)-(8):

- Continuity:

$$\frac{\partial U}{\partial X} + \frac{\partial V}{\partial Y} + \frac{\partial W}{\partial Z} = 0 \tag{3}$$

- Momentum

$$U\frac{\partial U}{\partial X} + V\frac{\partial U}{\partial Y} + W\frac{\partial U}{\partial Z} = -\frac{\partial P}{\partial X} + \frac{1}{Re}\left(\frac{\partial^2 U}{\partial X^2} + \frac{\partial^2 U}{\partial Y^2} + \frac{\partial^2 U}{\partial Z^2}\right) \tag{4}$$

$$U\frac{\partial V}{\partial X} + V\frac{\partial V}{\partial Y} + W\frac{\partial V}{\partial W} = -\frac{\partial P}{\partial Y} + \frac{1}{Re}\left(\frac{\partial^2 V}{\partial X^2} + \frac{\partial^2 V}{\partial Y^2} + \frac{\partial^2 V}{\partial Z^2}\right) + Ri\theta \tag{5}$$

$$U\frac{\partial W}{\partial X} + V\frac{\partial W}{\partial Y} + W\frac{\partial W}{\partial Z} = -\frac{\partial P}{\partial Z} + \frac{1}{Re}\left(\frac{\partial^2 W}{\partial X^2} + \frac{\partial^2 W}{\partial Y^2} + \frac{\partial^2 W}{\partial Z^2}\right) \tag{6}$$

- Thermal energy

$$U\frac{\partial \theta}{\partial X} + V\frac{\partial \theta}{\partial Y} + W\frac{\partial \theta}{\partial Z} = \frac{1}{Pr\,Re}\left(\frac{\partial^2 \theta}{\partial X^2} + \frac{\partial^2 \theta}{\partial Y^2} + \frac{\partial^2 \theta}{\partial Z^2}\right) \tag{7}$$

where the dimensionless variables are defined as:

$$(X, Y, Z) = \frac{(x, y, z)}{l}, (U, V, W) = \frac{(u, v, w)}{u_{in}}, P = \frac{p}{\rho u_{in}^2}, \theta = \frac{(T - T_{in})}{T_w - T_{in}} \tag{8}$$

where U, V, W are dimensionless velocity components along X, Y, Z directions, respectively, P and θ are dimensionless pressure and dimensionless temperature of fluid, respectively.

Reynolds number (Re), Grashof number (*Gr*), Richardson number (*Ri*) and Prandtl number (Pr) are written as follows:

$$\text{Re} = \frac{u_{in} D_h}{\nu}, Gr = \frac{g \beta_T \Delta T l^3}{\nu^2}, Ri \frac{Gr}{\text{Re}^2}, Rr = \frac{\nu}{\alpha} \tag{9}$$

where u_{in}, D_h, g, ν, β_T are inlet velocity flow, hydraulic diameter, gravitational acceleration, kinematic velocity, and volume expansion coefficient, respectively.

The relationship between Dean number and Reynolds number is determined from Eq. (10):

$$De = \frac{u_{in} D_h}{\nu} \sqrt{\frac{D_h}{R_c}} = \text{Re} \sqrt{\frac{D_h}{R_c}} \tag{10}$$

where R_c is the radius of curvature. For present geometry, $D_h / R_c = 0.066$, where $R_c = (R_1 + R_2)/2$.

The boundary conditions used for the flow and heat transfer configurations are presented:
- At inlet of channel: uniform velocity and constant temperature, i.e.,

$$U = 1, \ V = 0, \ W = 0, \ \theta = 0. \tag{11}$$

On channel walls: no-slip condition and constant temperature

$$U = 0, \ V = 0, \ W = 0, \ \theta = 1. \tag{12}$$

- At the outlet channel: Neumann boundary condition is used for flow velocity and temperature, i.e.,

$$\frac{\partial U}{\partial X} = 0, \ \frac{\partial V}{\partial X} = 0, \ \frac{\partial W}{\partial X} = 0 \frac{\partial \theta}{\partial X} = 0. \tag{13}$$

The local Nusselt number on cylinder surface is obtained by the expression:

$$Nu_l = \frac{hd}{k} = -\frac{\partial \theta}{\partial n_s} \tag{14}$$

where h and n_s are the local surface heat transfer coefficient and the normal direction to the wall surface. These local values on entire surfaces of duct were then averaged to obtain the average Nusselt number of a studied 180° curved duct.

$$Nu = \frac{1}{S} \int_s Nu_l ds \tag{15}$$

3 Solution methodology
The present study is performed by the package ANSYS-CFX that is developed by AEA technology. This commercial code uses a finite volume method to solve the governing equations subjected to aforementioned boundary conditions [19]. ANSYS-CFX converts the governing partial differential equations of momentum, continuity and energy into a system of discrete algebraic equations by discretizing the entire numerical domain. The steady-state laminar flow is selected for present governing equations; the source term in momentum equation (y-direction) originated due to the application of internal thermal buoyancy effect is added through (Function) feature of ANSYS-CFX. The high resolution discretization scheme is used for the spatial discretization of the convective terms, (SIMPLEC algorithm) a pressure-correction method of the type Semi-Implicit Method for Pressure-Linked Equations-Consistent is used as the pressure-velocity coupling schema.

The present grid has been generated using Gambit software. The grid points inside the entire computational domain are discretized in uniform manner with hexagonal elements combine with 1184000 and 1245621 nodes as it is illustrated in the Fig. 2. The grid number used in present work is chosen based on the grid independency study that is presented clearly in the Table 1.

4 Results and discussion
The obtained results are shown in term of streamlines and isotherms for different values of global flow and heat transfer quantities. The representative contours are illustrated at the cross-section of angle 0° and 90°. A longitudinal visualization of the streamlines and isotherms along the entire curved duct are also plotted.
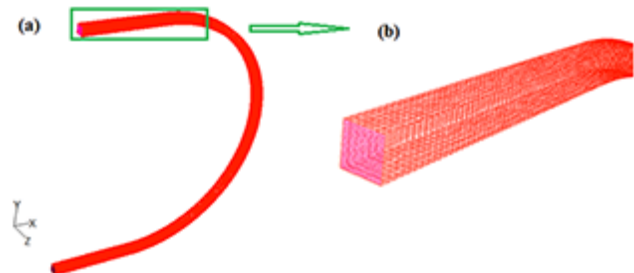

Fig. 2 Typical grids used for simulation

Table 1 Variation of average Nu versus grid element number

Mesh	Element	Nu	Error %
Mesh1	1120000	1.45024	0.01708
Mesh2	1152000	1.46732	0.00321
Mesh3	1168000	1.47053	0
Mesh4	1184000	1.47053	-

4.1 Numerical validation

A group of comprehensive numerical validation of Newtonian mixed and forced heat transfer on heated surface of obstacles confined in straight channelcan be found in our previous works of the second and fourth co-authors [20, 21]. Additional validation is presented here for Newtonian flow through a 180° curved channel of square cross-section as it is published in Helin et al. [22]. Fig. 3 shows the comparison of present result with that found by Helin et al. [22]. It is clearly observed that the size of vortices increases with increase in De number. Therefore, a good agreement is seen between the two results. A second additional quantitative test is also presented in the Fig. 4. The test shows a comparison between present result and the experimental result of Bara et al. [18]. Indeed, the figure presents an axial velocity profiles for different angular position of a curved channel of square cross-section at Dean number of 125. A good agreement is also detected between the results.

4.2 Flow patterns and isotherm contours

Figs. 5 and 6 show the streamlines at 0° and 90° cross-sectional positions of curved duct respectively. For each position, the streamlines are illustrated for three Dean number: $De = 125$, 137 and 150, and for the range of Richardson number of $Ri = 0$ to 2.

From those figures, it is shown that, at $Ri = 0$ (when there is no effect of thermal buoyancy) and at 0° cross-sectional position of the bend portion, the streamlines are observed to be stable for the three values of Dean number (125, 137 and 150), there is no apparition of Dean vortices.

On other hand, at 90° cross-sectional position, two large symmetric vortices form clearly in the square cross-section. Also, two additional symmetric vortices appear close to the outer wall of the channel and the size of additional vortices is observed to be increased with increase in the value of Dean number. This trend is in line with that observed for the experimental work of Bara et al. [18] and numerical work of Helin et al. [22]. Generation of vortices at the curved duct is due to the centrifugal force of the fluid flow through the bendsection. The colors are shown on the streamlines indicate the distribution of the dimensionless streamwise velocity; the red color is for the maximum value meanwhile, the blue color is for the minimum value. It is clear that, at 0° position, the maximum value of velocity is located at the center of cross-section. For the position 90° of bend section, the maximum velocity shifts towards the outer wall. This behavior substantiates the presence of centrifugal force at 90° position.

When the Richardson number increases from 0 to 2, complicated behaviors of flow patterns occur at cross-sectional positions of curved channel. At the 0° position, two large symmetric vortices dominate the square cross-section. Two additional symmetric vortices are seen to be formed close to inner wall. With gradual increases in Dean number and/or Richardson number, the additional vortices move towards the lateral walls. The presence of vortices at 0° cross-sectional position of bend section can be explained by the fact that as the Richardson number increases, the velocities of fluid particles on inner wall surface of bend portion increase and move towards the upward direction (where there is outer wall) then it causes
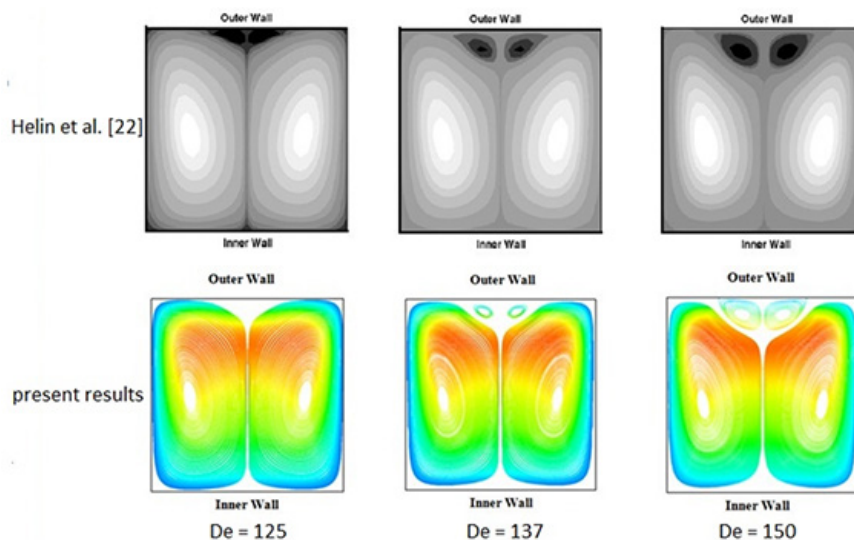

Fig. 3 Comparison of present results with Helin et al. [22] for De = 125, 137 and 150 for $\theta = 90°$

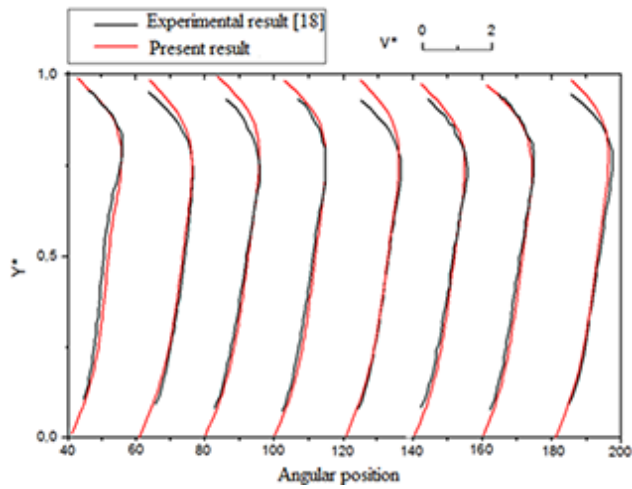**Fig. 4** Comparison of present results with Bara et al. [18]. For different angular position at De = 125

flow stagnation in the upper part of 0° cross-sectional position. Consequently, the flow velocity in lower part of 0° square section increases owing to mass conservation principle. The gradient velocity creates secondary flows. The velocity contours plotted at 0° position assure that the maximum value is near the inner wall meanwhile, the minimum is close to the outer wall.

For the 90° cross-sectional position, for three values of Dean number (125, 137 and 150), it is observed that the flow patterns become more complicated due to the combined influences of centrifugal force and thermal buoyancy. An increase in the value of Richardson number from 0 to 2 suppresses gradually the additional small vortices that were located closed to outer wall. It is also shown that the size of large vortices decreases with increasing Richardson number. Moreover, for Dean number of
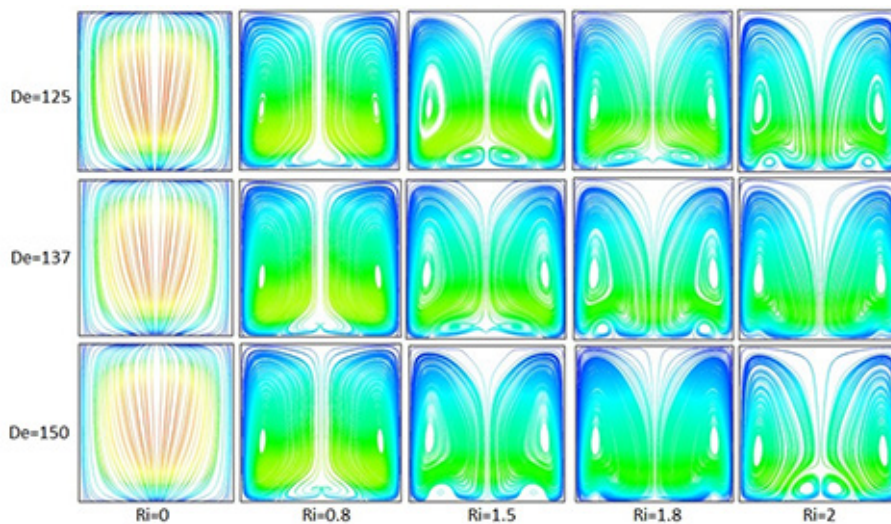

Fig. 5 Streamlines at the position 0° for De = 125, 137 and 150, for Ri = 0 to 2

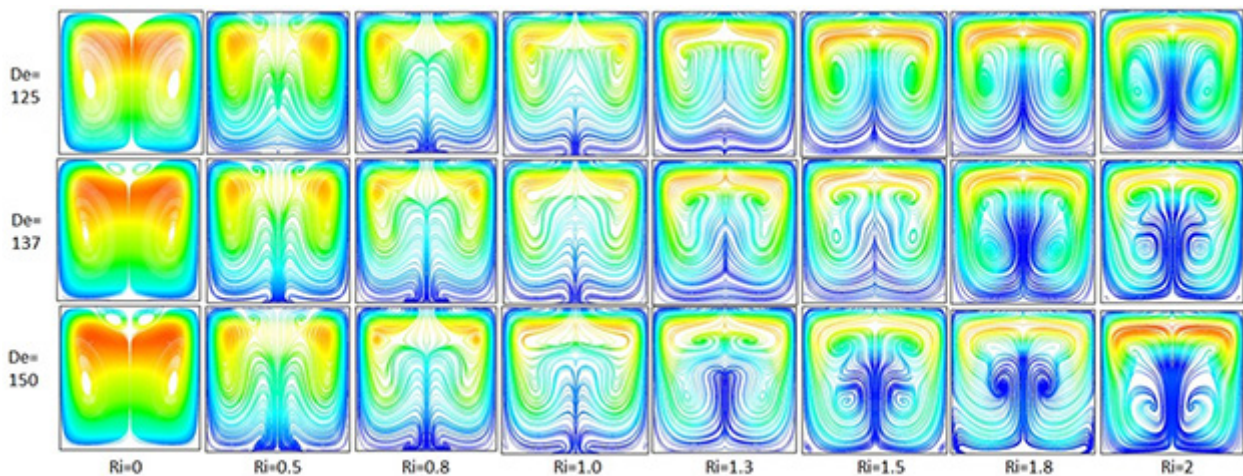**Fig. 6** Streamlines at the position 90° for De = 125, 137 and 150, for Ri = 0 to 2

$De = 125$, increase in Richardson number, the vortex center shifts progressively towards the outer channel wall initially and it moves back towards the inner wall. For $De = 137$ and 150, initially the vortex center moves also toward the outer wall with gradual increase in Richardson number then it divides into two vortices. Furthermore, for 90° square cross-sectional position, two very small vortices appear on inner wall of the channel, the size of vortices increases with increasing Dean number and their centers move progressively towards the lateral walls with increasing Richardson number. The velocity field shows

that the maximum streamwise velocity is near the outer wall for all values of Richardson number. The maximum velocity is also observed to be moved towards the lateral wall with increase in Richardson number.

Figs. 7 and 8 depict representative isotherm contours at 0° and 90° cross-sectional position for different values of Dean number and Richardson number. The isotherm contours show the same trend of physical phenomena detected from streamlines and velocity contours visualizations. At 0° position and without effect of thermal buoyancy, the isotherms have diffusion-type like uniformed circular
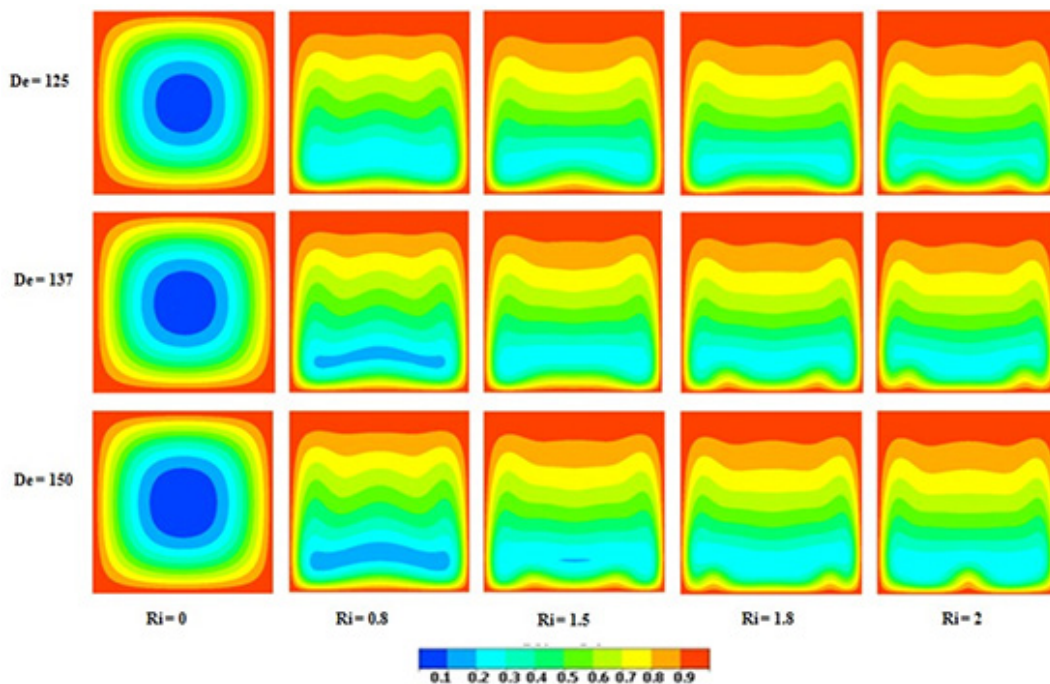

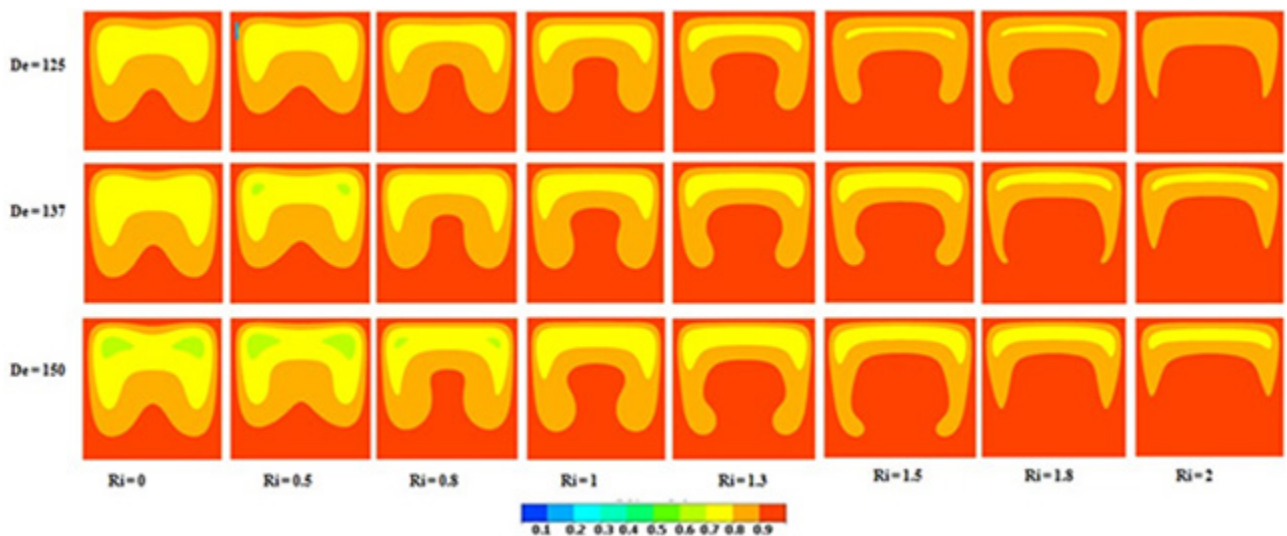**Fig. 7** Isotherms at the position 0° for De = 125, 137 and 150, for Ri = 0 to 2

Fig. 8 Isotherms at the position 90° for De = 125, 137 and 150, for Ri = 0 to 2

profiles around the square central position indicating the equal heat transfer rate of all cross-sectional square walls. For 90° position, the isotherms are crowded on the surface of outer wall hinting higher heat transfer rate of outer wall at 90° position compared to inner wall, this behavior is due to centrifugal force. It should be known that the progressive thinning of thermal boundary layer on wall surface shows an increase of heat transfer evacuation and the local Nusselt number to be increased progressively. The isotherms become non-uniform when the thermal buoyancy is added. At 0° cross-sectional position, for the three values of Dean number, more crowding of dimensionless temperature is found near to surface of the inner wall due to effect of gravitational effect. For fixed value of Richardson number, the isotherm clustering is observed to be increased with increasing in Dean number. At 90° position and for mixed convection, the crowing of isotherms is still close to outer surface of wall. Also, the lateral distributions of isotherms are observed to increase with increase in Dean number. Generally, the heat transfer rate at 0° position is greater than at 90°.

Fig. 9 depicts a longitudinal representative streamlines inside 180° curved duct for different values of Dean number and Richardson number. For all Dean number, and for $Ri = 0$, the streamlines are found to completely stable inside the channel and there is no counter rotating regions. The dimensionless velocity contours for the same conditions show that inside the upstream duct, the maximum value is located at the center, whereas, it is observed to move towards the outer wall inside the bend portion due to the centrifugal force. When the thermal buoyancy is considered, it is shown that by increasing the value of Richardson number, the flow starts to be instable progressively. Some closed steady contour rotating regions are observed to be appeared close to outer wall of half upper part of curved duct and others on inner wall of half down part of curved duct. The size of those regions increase along stream-wise and transverse direction with gradual increase in Richardson number and/or Dean number. The analyze of dimensionless velocity distribution shows that the maximum value of it is near to inner wall of bend section of duct up to the degree 80° where it moves towards the outer wall. Finally, it can be concluded that the influence of thermal buoyancy has a tendency to delay the effect of centrifugal force of flow through 180° curved channel of square cross section.
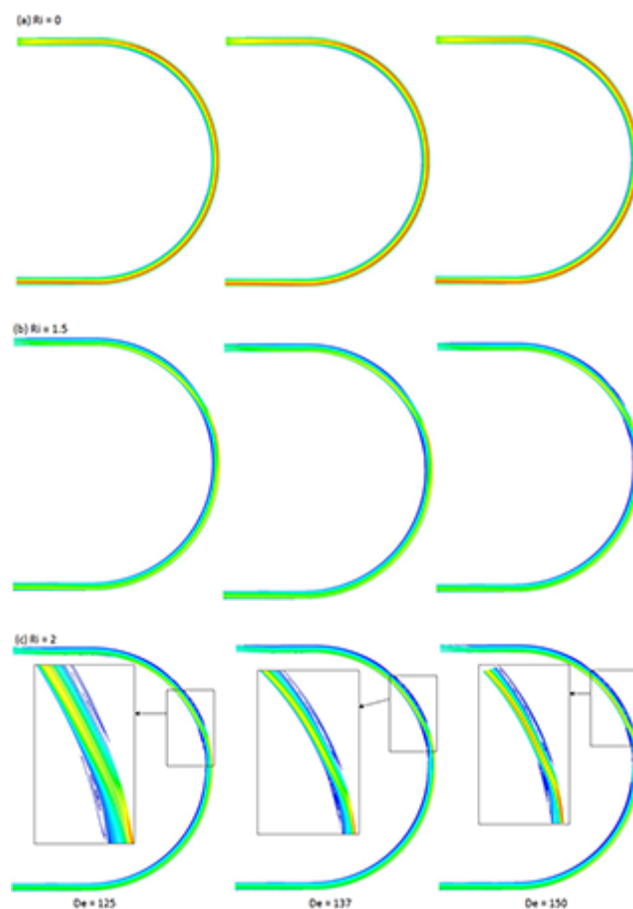

Fig. 9 Longitudinal streamline contours De = 125, 137 and 150, for Ri = 0, 1.5 and 2

4.3 Dimensionless velocity profiles

In order to present the developments of streamwise velocity at the square cross-sectional positions of 0° and 90° under the effect thermal buoyancy, Figs. 10 and 11 plot respectively the dimensionless velocity profiles of U_l along the symmetry axis of 0° and 90° for different values of Dean number and Richardson number. Fig. 10 depicts that for the three values of Dean number, the streamwise velocity is parabolic at the position 0° for $Ri = 0$. On other hand, the velocity profiles become clearly asymmetric when the thermal buoyancy is added. Generally, for all Dean number, the maximum values of streamwise velocity are near the inner wall at $r = 0.22H$, where r is the distance from inner to outer walls. From Fig. 11 it is clear that the velocity profiles are asymmetric for all values of Dean number at $Ri = 0$ and the streamwise velocity is maximum close to outer wall due to centrifugal force. It is also observed that the maximum value of velocity profile moves gradually
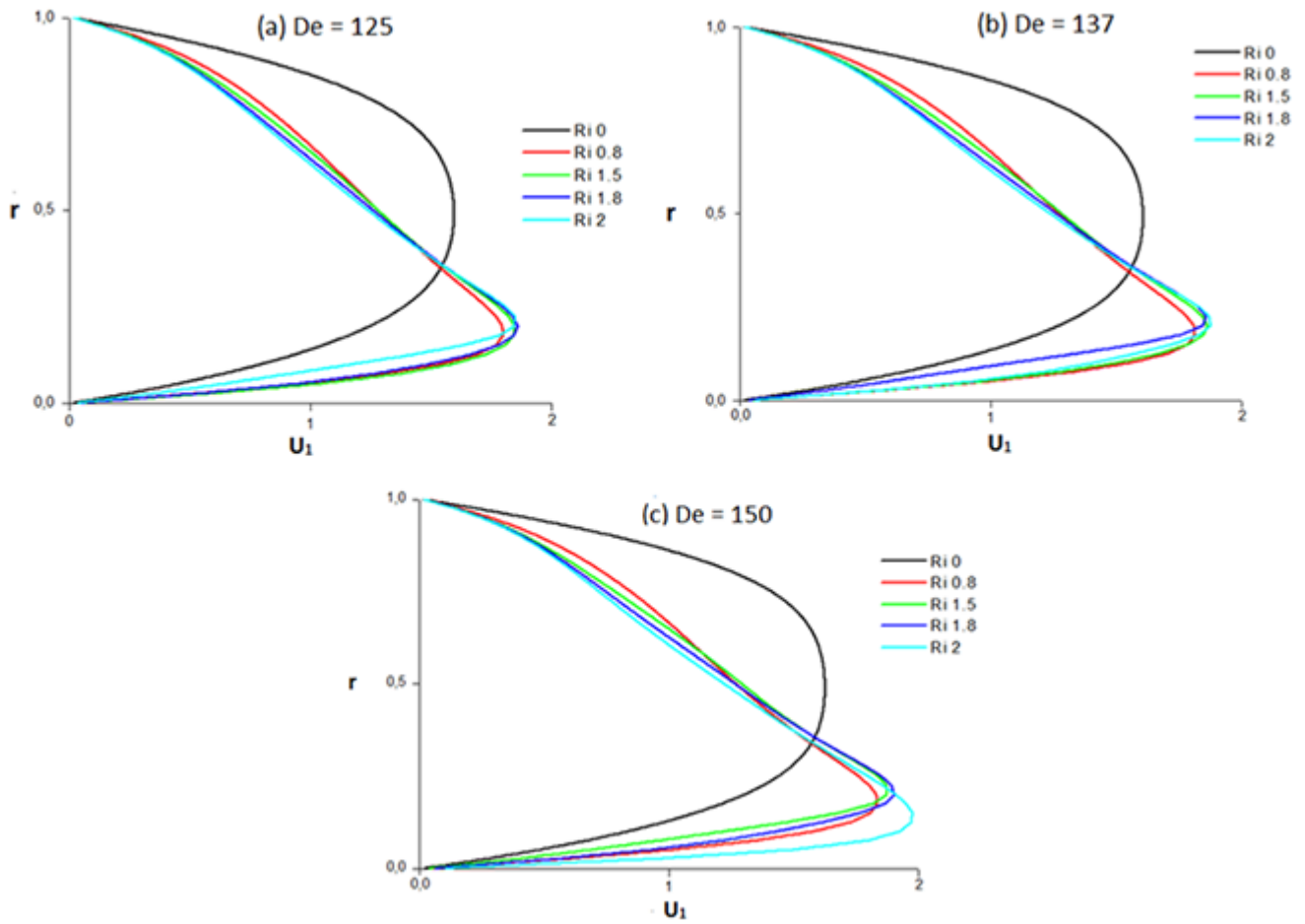
Fig. 10 Profiles of dimensionless streamwise velocity at 0° cross-sectional position for different Dean and Richardson numbers

to outer wall with increasing in Richardson number. Interesting distribution of streamwise velocity profiles is shown with Richardson number at the duct center channel of 90° cross-section. The streamwise velocity value is seen to decrease with gradual increase in Richardson number due to the presence of longitudinal counter-rotating region near the position 90° of bend portion.

4.4 Local Nusselt number

Figs. 12 and 13 show the variations of local Nusselt number along the inner, outer and lateral surfaces of 0° and 90° square cross-sectional positions respectively for different values of Dean number and Richardson number. At 0° position and for $Ri = 0$, the local Nusselt number has the same distribution along the surfaces. The maximum value is observed to be located at the center of each surface. The local Nusselt number maximum increases tightly with Dean number. Meanwhile, the local Nusselt number has an asymmetrical distribution when the thermal buoyancy is considered, Fig. 12 shows that along the

lateral surface and for all Dean number, the local Nusselt number increases with increasing Richardson number, the maximum value of Nusselt near the inner wall. On outer surface, the local Nusselt number decreases gradually with increasing Richardson number. Interesting distribution of local Nusselt number is observed along the inner surface versus Richardson number. It is observed that depending upon the value of Richardson number, the local Nusselt number may increase or decrease thereby indicating a non-monotonic relationship between the local Nusselt number and Richardson number. It is clearly shown that the reduction of local Nusselt number is due to existence of counter rotating regions that decrease the evacuation of heat transfer from the channel wall to fluid flow. From Fig. 13, it is clear that the local Nusselt number has an asymmetrical distribution along the surfaces of 90° position for $Ri = 0$ (forced convection), the maximum values of local Nusselt number are along the outer surface and along the parts of lateral surfaces that are closed to outer surface. Meanwhile, the minimum values are along the
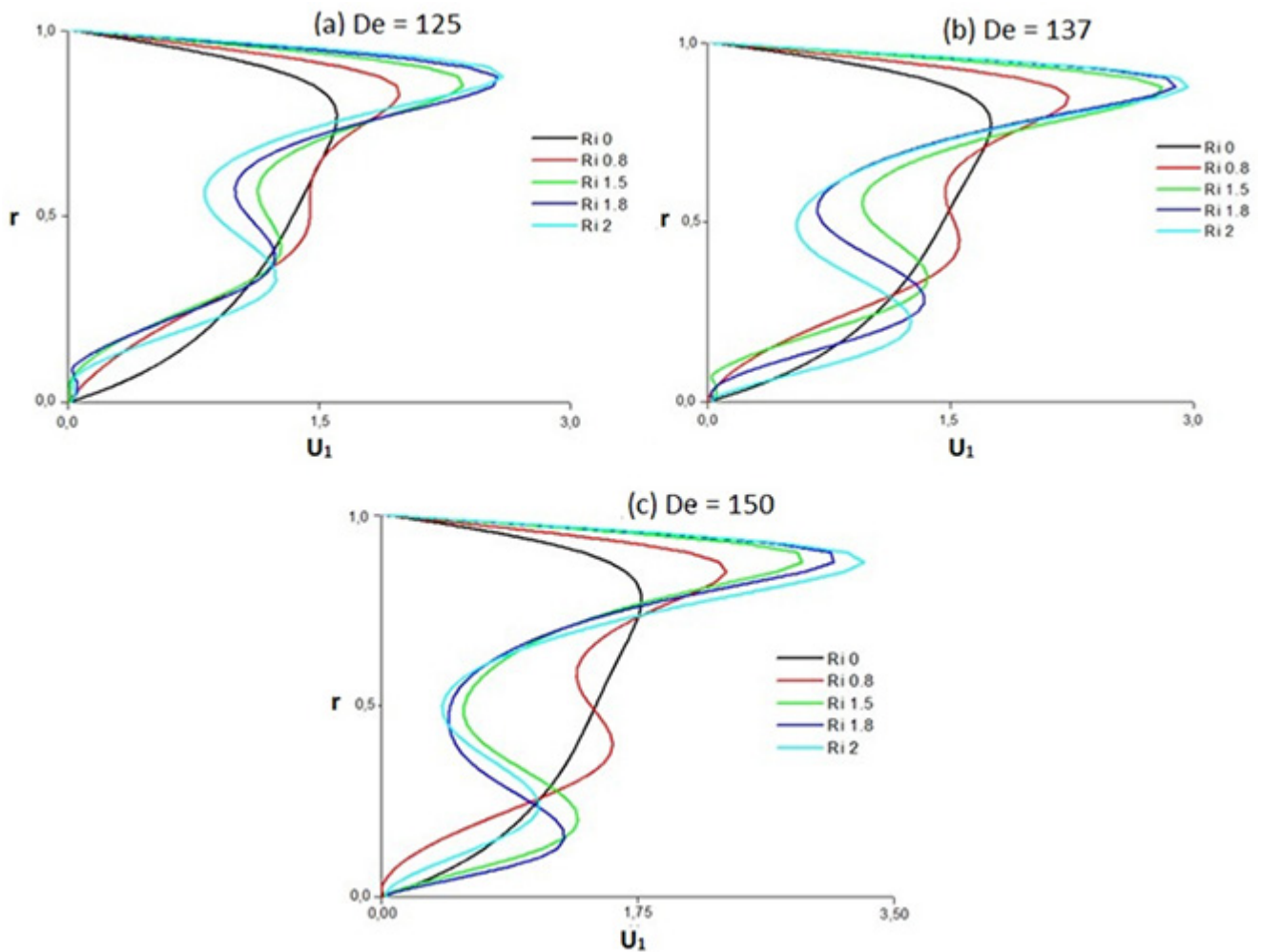
Fig. 11 Profiles of dimensionless streamwise velocity at 90° cross-sectional position for different Dean and Richardson numbers

inner surface, this is due to effect of centrifugal force that increases the flow velocity near the outer wall and according, an increasing of heat transfer evacuation. The values of local Nusselt number increase with increase in the value of Dean number. For Richardson number different from zero (mixed convection), new distribution form of local Nusselt number is observed with respect to Richardson number. In the whole, the thermal buoyancy has a tendency to increase the local Nusselt number along the outer and lateral surfaces of 90° position showing a non-monotonic evolution between the local Nusselt number and Richardson number. On other hand, along the inner surface of 90° square position and for the range of Richardson number of $Ri = 0$ to 2, adding thermal buoyancy to studied geometry decreases the heat transfer for the Dean number of $De = 125$, meanwhile, it enhances gradually the heat transfer rate for Dean number of $De = 137$ and 150. Finally, for all values of Dean number and Richardson

number, there is no value of local Nusselt number at the four corners of square cross-sectional positions.

4.5 Average Nusselt number
Fig. 14 shows the variation of average Nusselt number of the entire 180° curved duct for three values of Dean number ($De = 125$, 137 and 150) and for the range of Richardson number limited between $Ri = 0$ and 2. It is shown that for all values of Richardson number increase in Dean number increases the heat transfer rate. Furthermore, at fixed value of Dean number, a gradual increase in Richardson number decreases the average Nusselt number of the 180° curved channel.

5 Conclusion
The present research is conducted to investigate the flow through a 180° curved duct of square cross-section under the effect of thermal buoyancy. The numerical simulations are carried out for the range of following conditions as:
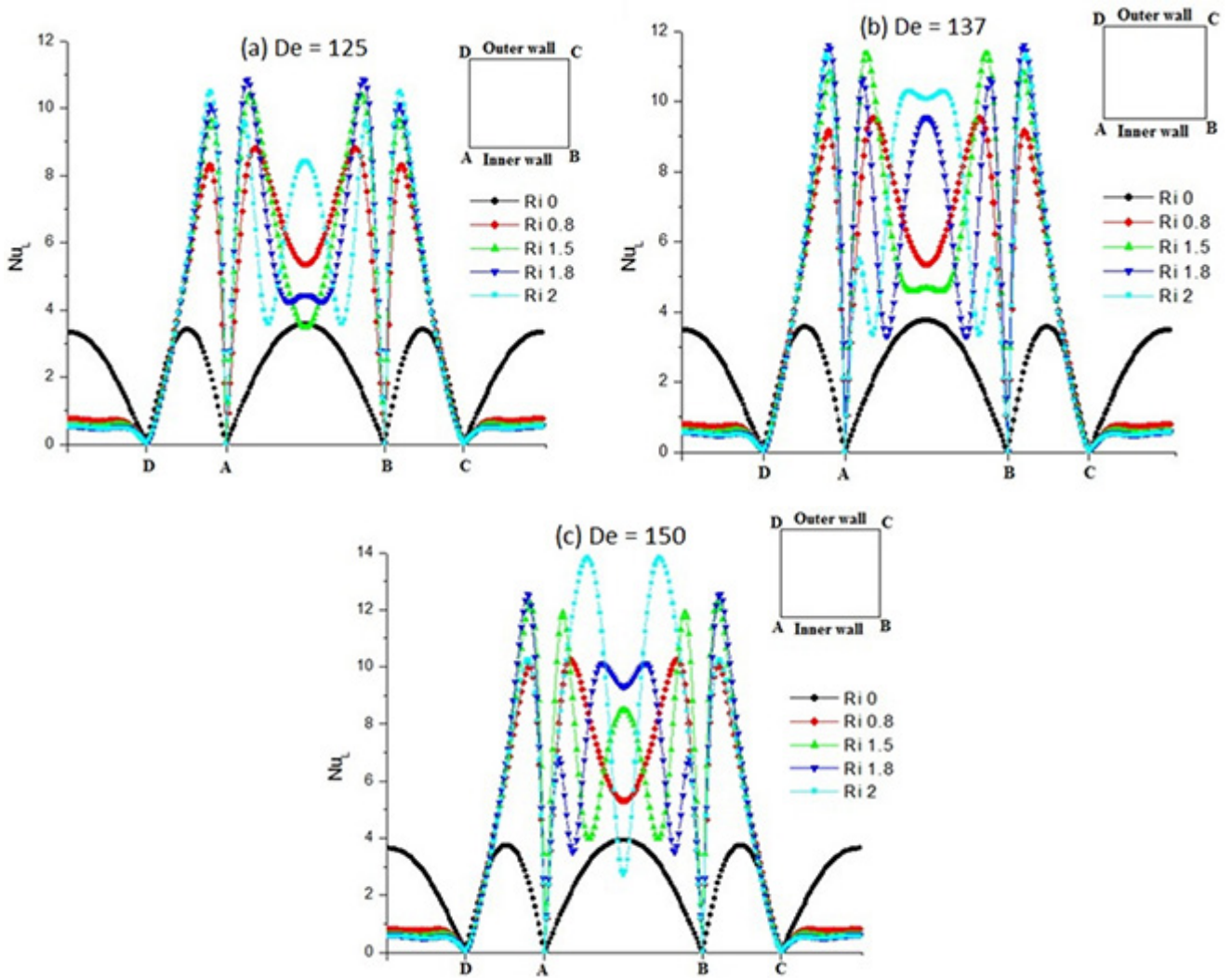
Fig. 12 Variation of local Nusselt number at 0° cross-sectional position for different Dean and Richardson numbers

De = 125 to 150, Ri = 0 to 2 and Pr = 1. The study provided the flow behavior and its effect on heat transfer rate at the 0° and 90° cross-sectional position of bend portion of the channel. The average Nusselt of the entire curved channel is also calculated. The principal finding can be summarized as:

- The thermal buoyancy has a tendency to create a new sort of dean vortices especially at 0° position of bend portion of the 180° curved channel.
- Increase in the value of Dean number increases the effect of centrifugal force and accordingly increase in the instability of the flow in bend section.
- The adding of the thermal buoyancy decreases considerably the effect of centrifugal force in the upper part of bend section.
- The gradual increase in buoyancy strength suppresses progressively the small additional Dean vortices that are close the outer wall of 90° cross-sectional position.

- Introducing of thermal buoyancy generates some longitudinal counter rotating zones and the size of those zones is observed to be increased with the Dean and/or Richardson numbers.
- The local Nusselt number along the lateral surfaces of square cross-sectional positions of 0° and 90° increases with introducing the thermal buoyancy.
- The Local Nusselt number distribution along the inner wall of 0° position increases with adding the thermal buoyancy meanwhile, it decreases along the outer surface.
- Generally, it is can be concluded that increase in Dean number increases the average Nusselt number of 180° curved duct for all values of Richardson number. On other hand, at fixed value of Dean number, increases in Richardson number decreases the heat transfer rate inside the 180° curved duct.
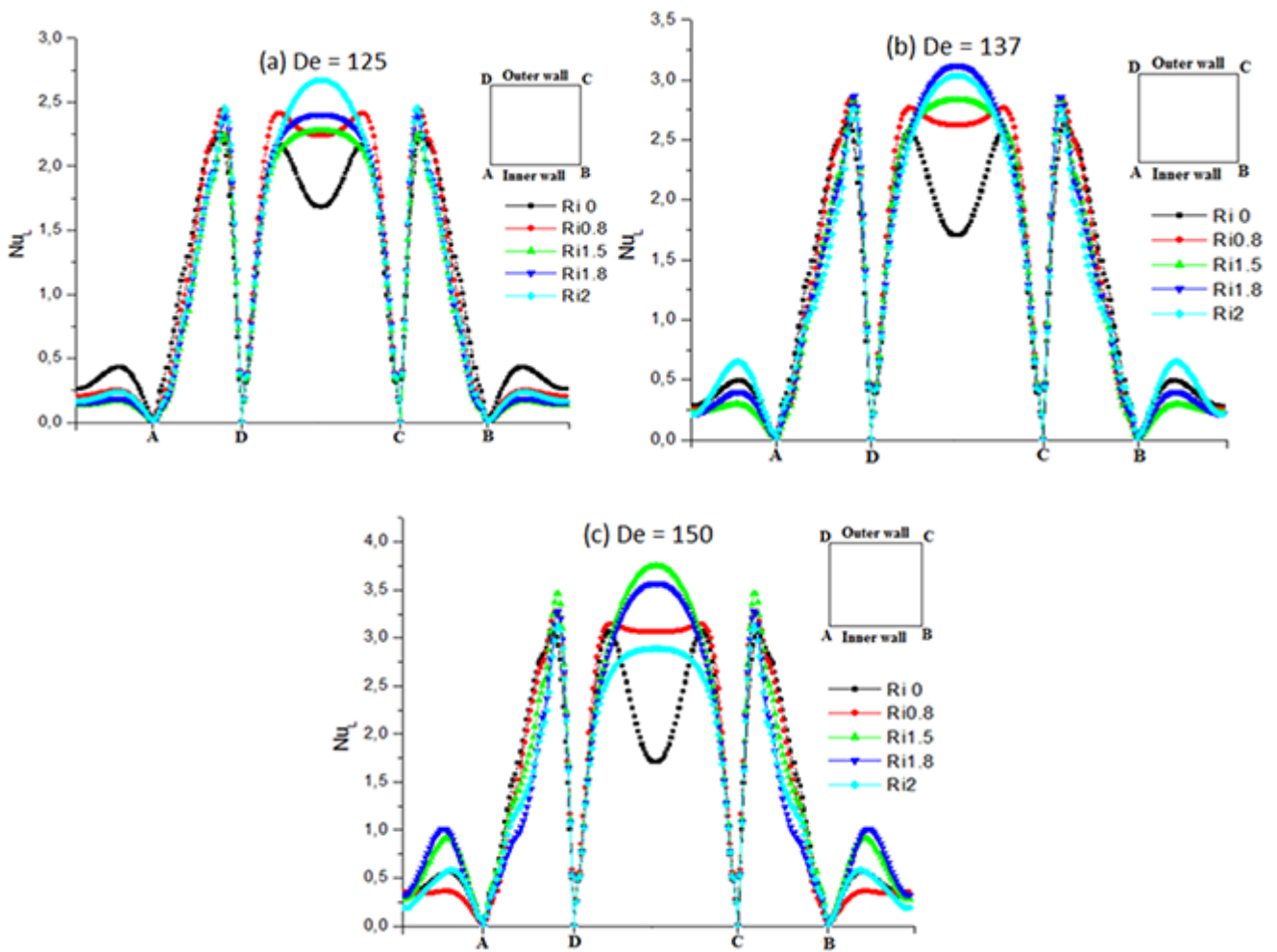
Fig. 13 Variation of local Nusselt number at 90° cross-sectional position for different Dean and Richardson numbers
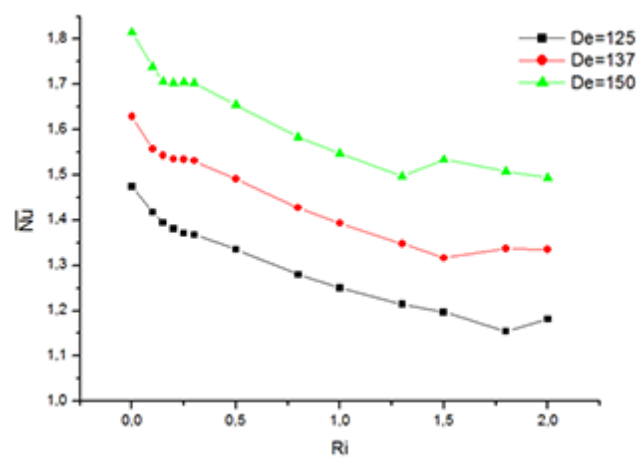

Fig. 14 Variation of average Nusselt number of the entire 180 curved channel for different Dean and Richardson numbers

References

[1] Finlay, W. H., Nandakumar, K. "Onset of two-dimensional cellular flow in finite curved channels of large aspect ratio", Physics of Fluids A: Fluid Dynamics, 2(7), pp. 1163–1174, 1990.
https://doi.org/10.1063/1.857617

[2] Dean, W. R. "Note on the motion of fluid in a curved pipe", The London, Edinburgh, and Dublin Philosophical Magazine and Journal of Science, 4(20), pp. 208–223, 1927.
https://doi.org/10.1080/14786440708564324

[3] Fellouah, H., Castelain, C., Ould-El-Moctar, A., Peerhossaini, H. "The Dean instability in power-law and Bingham fluids in a curved rectangular duct", Journal of Non-Newtonian Fluid Mechanics, 165(3-4), pp. 163–173, 2010.
https://doi.org/10.1016/j.jnnfm.2009.10.009

[4] Fellouah, H., Castelain, C., Ould-El-Moctar, A., Peerhossaini, H. "A criterion for detection of the onset of Dean instability in Newtonian fluids", European Journal of Mechanics – B/Fluids, 25(4), pp. 505–531, 2006.
https://doi.org/10.1016/j.euromechflu.2005.11.002

[5] Jarrahi, M., Castelain, C., Peerhossaini, H. "Secondary flow patterns and mixing in laminar pulsating flow through a curved pipe", Experiments in Fluids, 50(6), pp. 1539–1558, 2010.
https://doi.org/10.1007/s00348-010-1012-z

[6] Rout, S., Mukherjee, A., Barik, A. K., Satapathy K. P. "Laminar Fluid Flow and Heat Transfer Characteristics of Al2O3 Nanofluid in 180-degree Return Bend Pipe", International Journal of Control Theory and Applications, 10(7), pp. 81–89, 2017.

[7] Norouzi, M., Kayhani, M. H., Shu, C., Nobari, M. R. H. "Flow of second-order fluid in a curved duct with square cross-section", Journal of Non-Newtonian Fluid Mechanics, 165(7-8), pp. 323–339, 2010.
https://doi.org/10.1016/j.jnnfm.2010.01.007

[8] Malheiro, J. M., Oliveira, P. J., Pinho, F. T. "Parametric study on the three-dimensional distribution of velocity of a FENE-CR fluid flow through a curved channel", Journal of Non-Newtonian Fluid Mechanics, 200, pp. 88–102, 2013.
https://doi.org/10.1016/j.jnnfm.2012.12.007

[9] Papadopoulos, P. K., Hatzikonstantinou, P. M. "Numerical study of laminar fluid flow in a curved elliptic duct with internal fins", International Journal of Heat and Fluid Flow, 29(2), pp. 540–544, 2008.
https://doi.org/10.1016/j.ijheatfluidflow.2007.11.003

[10] Li, Y., Wang, X., Zhou, B., Yuan, S., Tan, S. K. "Dean instability and secondary flow structure in curved rectangular ducts", International Journal of Heat and Fluid Flow, 68, pp. 189–202, 2017.
https://doi.org/10.1016/j.ijheatfluidflow.2017.10.011

[11] Dai, Z.-P., Yin, Z.-Q. "Flow and deposition characteristics of nanoparticles in a 90° square bend", Thermal Science, 19(4), pp. 1235–1238, 2015.
https://doi.org/10.2298/TSCI1504235D

[12] Nayak, B. B., Chatterjee, D., Mullick, A. N. "Numerical prediction of flow and heat transfer characteristics of water-fly ash slurry in a 180° return pipe bend", International Journal of Thermal Sciences, 113, pp. 100–115, 2017.
https://doi.org/10.1016/j.ijthermalsci.2016.11.019

[13] Soltanipour, H., Choupani, P., Mirzae, I. "Numerical analysis of heat transfer enhancement with use of nonofluid and longitudinal ribs in curved duct", Thermal Science, 16(2), pp. 469–480, 2012
https://doi.org/10.2298/TSCI110719028S

[14] Nobari, M. R. H., Mehrabani, M. T. "A numerical study of fluid flow and heat transfer in eccentric curved annuli", International Journal of Thermal Sciences, 49(2), pp. 380–396, 2010.
https://doi.org/10.1016/j.ijthermalsci.2009.07.003

[15] Ko, T. H. "Numerical investigation on laminar forced convection and entropy generation in a curved rectangular duct with longitudinal ribs mounted on heated wall", International Journal of Thermal Sciences, 45(4), pp. 390–404, 2006.
https://doi.org/10.1016/j.ijthermalsci.2005.06.005

[16] Chandratilleke, T. T., Nadim N., Narayanaswamy, R. "Vortex structure-based analysis of laminar flow behaviour and thermal characteristics in curved ducts", International Journal of Thermal Sciences, 59, pp. 75–86, 2012.
https://doi.org/10.1016/j.ijthermalsci.2012.04.014

[17] Fayçal, B., Laidoudi, H., Bouzit, M. "Simulation of power-law fluids and mixed convection heat transfer inside of curved duct", Defect and Diffusion Forum, 378, pp. 113–124, 2017.
https://doi.org/10.4028/www.scientific.net/DDF.378.113

[18] Bara, B., Nandakumar, K., Masliyah, J. H. "An experimental and numerical study of the Dean problem: flow development towards two-dimensional multiple solutions", Journal of Fluid Mechanics, 244, pp. 339–376, 1992.
https://doi.org/10.1017/S0022112092003100

[19] ANSYS CFX-11.0 User Manual, ANSYS Inc., Canonsburg, USA, November 2006.

[20] Laidoudi, H., Bouzit, M. "Mixed convection in Poiseuille fluid from an asymmetrically confined heated circular cylinder", Thermal Science, 22(2), pp. 821–834, 2018.
https://doi.org/10.2298/TSCI160424172L

[21] Laidoudi, H. "Suppression of flow separation of power-law fluids around a confined circular cylinder by superimposed thermal buoyancy", Mechanics, 23(2), pp. 220–227, 2017.
https://doi.org/10.5755/j01.mech.23.2.14342

[22] Helin, L., Thais, L., Mompean, G. "Numerical simulation of viscoelastic Dean vortices in a curved duct", Journal of Non-Newtonian Fluid Mechanics, 156(1-2), pp. 84–94, 2009.
https://doi.org/10.1016/j.jnnfm.2008.07.002

[23] Girish, N., Makinde, O. D., Sankar, M. "Numerical investigation of developing natural convection in vertical double-passage porous annuli", Defect and Diffusion Forum, 387, pp. 442–460, 2018.
https://doi.org/10.4028/www.scientific.net/DDF.387.442

[24] Sankar, M., Kiran, S., Ramesh, G. K., Makinde, O. D. "Natural convection in a non-uniformly heated vertical annular cavity", Defect and Diffusion Forum, 377, pp. 189–199, 2017.
https://doi.org/10.4028/www.scientific.net/DDF.377.189